SUPPLEMENTAL DATA

Supplemental Methods

Flow cytometry

For mouse flow cytometry, mouse femurs and tibias were dissected and crushed in PBS containing 2% FBS. Bone marrow cells were transferred through a 40 µm cell strainer into a 50 ml tube and centrifuged at 500xg, 4°C for 5 min. Cells were incubated for 30 min at 4ºC with the following fluorochrome-conjugated antibodies: anti-CD71 APC (RI7217; 1:200), anti-Ter-119 APC/Cy7 (TER119; 1:200), anti-CD44 PE (IM7; 1:200), anti-Ly-6G/Ly-6C (Gr-1) PerCP (RB6-8C5; 1:200), anti-CD115 (CSF-1R) PE/Cy7 (AFS98; 1:200), anti-F4/80 BV510 (BM8; 1:100) all from Biolegend and anti-FPN AF647 (Novus Biologicals, cat # NBP1-21502AF647; 1:100). Flow cytometric quantification of the labile iron pool (LIP) was achieved with Phen Green™ SK diacetate (#P14313, Invitrogen™). Prior to use, Phen Green SK was dissolved in dimethylsulfoxide (DMSO). Bone marrow cells were incubated 5 min RT with Red Blood Cell Lysis Buffer (#420301, Biolegend), and centrifuged 500xg, 4°C for 5 min. Cells were incubated for 15 min at 37ºC with 5uM Phen Green™ SK diacetate diluted with Hank's balance salt solution (HBSS, Gibco, #14175). Staining for intracellular markers was performed using Foxp3 Transcription Factor Staining Buffer Set (Thermo Fisher Scientific, #00-5523-00). Isolated bone marrow cells were first stained for cell surface markers with the following fluorochrome-conjugated antibodies: anti-CD45.1 APC (A20, 1:100), and anti-CD71 FITC (RI7217, 1:200) all from Biolegend. Cells were then fixed and permeabilized with Fix:Perm solution for 30 min at RT. Cells were centrifuged at 500xg, 4ºC for 5 min and washed with the Permeabilization buffer. Cells were incubated with anti-Ki-67 Pe-Cy7 antibody (16A8, Biolegend) for 30 min at RT (3ul antibody diluted in 100ul of permeabilization buffer). Live and dead cells were distinguished using 4,6-diamidino-2-phenylindole (DAPI, Invitrogen). Calibrite Beads (BD Biosciences) were used to determine absolute cell counts (3). Cells were analyzed with a flow cytometer BD FACSCANTO II (BD Biosciences) and data were analyzed with FlowJo.

For human flow cytometry, BM aspirates were processed according to EuroFlow recommendations and using the following antibodies: anti-CD45 PacO (clone HI30) from Molecular Probes, anti-CD36 FITC (clone FA6.152), anti-CD117 APC or PE-Cy7 (clone 104D2D1) and anti-CD105 PE (clone IG2) from Beckman Coulter, anti-CD71 APC (clone M-A712) and anti-CD34 PerCP-Cy5.5 (clone 8G12) from BD Biosciences and HLA-DR PB (clone L243) from Biolegend. Cells were analyzed with a flow cytometer BD FACSCANTO II (BD Biosciences). Analysis of human BM erythropoiesis was performed as described in (4) using the software InfinicytTM (Cytognos S.L.).

Quantitative polymerase chain reaction (qPCR)

Liver fragments were homogenized in NZYol (NZYTech, Lisbon, Portugal). Hip bones were crushed in ice-cold PBS. The cell suspension was filtered through a 40 µm nylon strainer (BD Falcon) to a 50 ml tube and centrifuged at 500×g for 5 min at 4°C. Total RNA was extracted using NZYol (NZYTech,

Lisbon, Portugal), followed by DNase treatment (Turbo DNA-free kit) (Life Technologies, Carlsblad, CA, USA). RNA integrity was assessed with an Experion Automated Electrophoresis System (Bio-Rad, Hercules, CA, USA). First-strand cDNA was prepared from 2 µg RNA using the NZY First-Strand cDNA Synthesis Kit (NZYTech, Lisbon, Portugal) with an oligo$(dT)_{18}$ primer. Relative gene expression levels were quantified using a CFX384 Real-Time PCR Detection System (Bio-Rad, Hercules, CA, USA). Primer sequences are listed in Supplementary Methods. All reactions were performed in a total volume of 10 µl with iTaq™ Universal SYBR Green Supermix. The amplification protocol consisted of denaturation at 95°C for 3 min 30 s and 40 cycles of 95°C for 20 s, and 59°C for 30 s. The relative quantity of each transcript was estimated by the $2^{-\Delta Ct}$ method, after normalization against the averaged Ct of two endogenous control genes, Hypoxanthine phosphoribosyltransferase 1 (Hprt1) and beta Actin (Actb).

Primer sequences:

Gene ID	Forward primer sequence (5'-3')	Reverse primer sequence (5'-3')
Actb	GGCGGACTGTTACTGAGCTGCGTTT	AAAGCCATGCCAATGTTGTCTCTT
Bmp6	TCCCCACATCAACGACACCA	TCCCCACCACACAGTCCTTG
Erfe	ACTACCTGCCCGAAGTTGAG	TTGTGCTGGCAGAGAGACTG
Hprt1	AGATGGGAGGCCATCACATTGT	ATGTCCCCCGTTGACTGATCAT

Perls staining

Femurs were fixed in neutral formalin 10%, incubated in EDTA-based decalcifying solution for 48 h and embedded in paraffin. Spleen samples were fixed in neutral formalin 10% and embedded in paraffin. Following deparaffinization with xylene and hydration by a passage through a grade of alcohols, 3 µm-thick spleen and 4 µm-thick femur sections were stained with Perls' Prussian blue reaction for ferric iron at IPATIMUP Diagnostics. All slides were examined by the same observer (TLD), in a blind manner.

Non-heme iron quantification

Non-heme iron content in spleen and liver samples was measured by the bathophenantroline method as described before (5).

Non-transferrin bound iron (NTBI) determination

NTBI determinations were carried out by the ultracentrifugation assay first described by Singh et al.(6) Serum samples (90 µl) were treated with 10 µl of an 800 mM NTA solution at pH 7.0 and were allowed to incubate for 30 minutes at room temperature. The mixture was then ultra-filtered at 10000xg and 4ºC for 1 hour, using 10 kDa molecular weight cut-off Amicon Ultra 0.5 ml filtration units (Millipore).

Iron content was subsequently measured in the ultra-filtrate by the colorimetric ferrozine assay adapted to a 96-microwell plate format(7, 8). 50 µl sample was mixed with 20 µl 4 mM ascorbic acid solution prepared in formic acid (0.2 M at pH 3) and allowed to incubate in the dark at room temperature. After 5 min, 25 µl 1 mM ferrozine reagent prepared in formic acid solution was added and the incubation was allowed to proceed for further 30 min. Iron concentration is read from a standard curve after determination of the solution absorbance at 562 nm. Standard iron solutions (0–10 µM) were prepared in 80 mM NTA and were analysed by using the same procedures as with serum samples.

Electron microscopy and EDS

The transmission electronic microscopy and energy-dispersive X-ray spectroscopy (EDS) analysis were performed at the HEMS core facility at i3S, University of Porto, Portugal with the assistance of Ana Rita Malheiro e Rui Fernandes and according to previously published methods (9). Femoral epiphysis samples were fixed by immersion in 2.5% glutaraldehyde and 2% paraformaldehyde in 0.1M sodium cacodylate buffer (pH 7.4) solution for 5 days and subsequently incubated in EDTA-based decalcifying solution (MoL-Decalcifier) for 48h. After washing and two hours in post-fixating 2% osmium tetroxide in 0.1M sodium cacodylate buffer (pH 7.4) solution, tissues were washed in buffer, incubated with 1% Uranyl acetate overnight, washed in buffer and dehydrated through a graded series of ethanol, and embedded in Epon (EMS). Semithin sections (approximately 0.5 µm thick), stained with toluidine blue and methylene blue, were used to search for areas of interest. Ultrathin sections were cut at 50 nm and prepared on a RMC Ultramicrotome (PowerTome, USA) using a diamond knife and recovered to 200 mesh copper grids, followed by double contrast method with 2% uranyl acetate and saturated lead citrate solution. Visualization was performed at 80 kV in a (JEOL JEM 1400 microscope, Japan) and digital images were acquired using a CCD digital camera Orious 1100 W (Tokyo, Japan). For Energy-dispersive X-ray spectroscopy (EDS) analysis, unstained sections were mounted on formvar/carbon film-coated mesh nickel grids and a beryllium holder (EM-21150, Jeol Ltd.) was used. An X-Max 80 mm2 (Oxford Instruments, Bucks, England) operated at 120 kV was coupled to the microscope.

TCGA data analysis

RSEM (RNA-Seq by Expectation Maximization) (10) scaled expression values for TCGA were downloaded from the GDAC Firehose website (11). Counts were normalised to transcripts-per-million (TPM) values with a pseudo-count of 2. Entrez gene IDs were mapped to HGNC gene symbols using the biomaRt R package (version 2.42.0) (12) and collapsed to unique values per gene symbol by selecting the most variable entrez ID among all samples for each gene symbol. Primary tumour samples were selected using the TCGAbiolinks R package (version 2.14.0) (13) and were matched with clinical information from the TCGA Pan-Cancer Clinical Data Resource (14). The ratio of TPM

values between the FTH1 and FTL genes was used to fit Kaplan-Meier and Cox regression models for the TCGA LAML cohort using the survival R package (version 3.1-8) (15).

RNA-seq data analysis

Transcriptome analysis were performed on previously published data GSE105159 (1). FeatureCounts (version 1.34.7) was used for read counting after which differential gene expression analysis was performed using Voom-LIMMA packages (limma version 3.40.6)(16-18).

Statistical analysis

Data were analyzed using GraphPad Prism (GraphPad Software, CA, USA) and SPSS Statistics (IBM). Unpaired t-test was used to compare group means. One-way ANOVA with post hoc Tukey test or Bonferroni correction was used for multiple comparisons. For survival analysis, the log-rank test was performed. Differences were considered significant when $p < 0.05$ (*$p < 0.05$, **$p < 0.01$, ***$p < 0.001$).

References (methods)

1. Duarte D, Hawkins ED, Akinduro O, Ang H, De Filippo K, Kong IY, et al. Inhibition of Endosteal Vascular Niche Remodeling Rescues Hematopoietic Stem Cell Loss in AML. *Cell Stem Cell.* 2018;22(1):64-77 e6.
2. Saito Y, Chapple RH, Lin A, Kitano A, and Nakada D. AMPK Protects Leukemia-Initiating Cells in Myeloid Leukemias from Metabolic Stress in the Bone Marrow. *Cell Stem Cell.* 2015;17(5):585-96.
3. Hawkins ED, Hommel M, Turner ML, Battye FL, Markham JF, and Hodgkin PD. Measuring lymphocyte proliferation, survival and differentiation using CFSE time-series data. *Nat Protoc.* 2007;2(9):2057-67.
4. Mello FV, Land MGP, Costa ES, Teodosio C, Sanchez ML, Barcena P, et al. Maturation-associated gene expression profiles during normal human bone marrow erythropoiesis. *Cell Death Discov.* 2019;5:69.
5. Neves JV, Olsson IA, Porto G, and Rodrigues PN. Hemochromatosis and pregnancy: iron stores in the Hfe-/- mouse are not reduced by multiple pregnancies. *Am J Physiol Gastrointest Liver Physiol.* 2010;298(4):G525-9.
6. Singh S, Hider RC, and Porter JB. A direct method for quantification of non-transferrin-bound iron. *Anal Biochem.* 1990;186(2):320-3.
7. Carter P. Spectrophotometric determination of serum iron at the submicrogram level with a new reagent (ferrozine). *Anal Biochem.* 1971;40(2):450-8.
8. Evans RW, Rafique R, Zarea A, Rapisarda C, Cammack R, Evans PJ, et al. Nature of non-transferrin-bound iron: studies on iron citrate complexes and thalassemic sera. *J Biol Inorg Chem.* 2008;13(1):57-74.
9. Pinto JP, Arezes J, Dias V, Oliveira S, Vieira I, Costa M, et al. Physiological implications of NTBI uptake by T lymphocytes. *Frontiers in pharmacology.* 2014;5:24.
10. Li B, and Dewey CN. RSEM: accurate transcript quantification from RNA-Seq data with or without a reference genome. *BMC Bioinformatics.* 2011;12:323.
11. Center BITGDA. Analysis-ready standardized TCGA data from Broad GDAC Firehose 2016_01_28 run. 2016.

12. Durinck S, Spellman PT, Birney E, and Huber W. Mapping identifiers for the integration of genomic datasets with the R/Bioconductor package biomaRt. *Nature protocols.* 2009;4(8):1184.
13. Colaprico A, Silva TC, Olsen C, Garofano L, Cava C, Garolini D, et al. TCGAbiolinks: an R/Bioconductor package for integrative analysis of TCGA data. *Nucleic acids research.* 2016;44(8):e71-e.
14. Liu J, Lichtenberg T, Hoadley KA, Poisson LM, Lazar AJ, Cherniack AD, et al. An Integrated TCGA Pan-Cancer Clinical Data Resource to Drive High-Quality Survival Outcome Analytics. *Cell.* 2018;173(2):400-16 e11.
15. Therneau T. 2015.
16. Liao Y, Smyth GK, and Shi W. featureCounts: an efficient general purpose program for assigning sequence reads to genomic features. *Bioinformatics.* 2014;30(7):923-30.
17. Liao Y, Smyth GK, and Shi W. The R package Rsubread is easier, faster, cheaper and better for alignment and quantification of RNA sequencing reads. *Nucleic acids research.* 2019;47(8):e47-e.
18. Law CW, Chen Y, Shi W, and Smyth GK. voom: Precision weights unlock linear model analysis tools for RNA-seq read counts. *Genome biology.* 2014;15(2):R29.

SUPLEMENTAL FIGURES

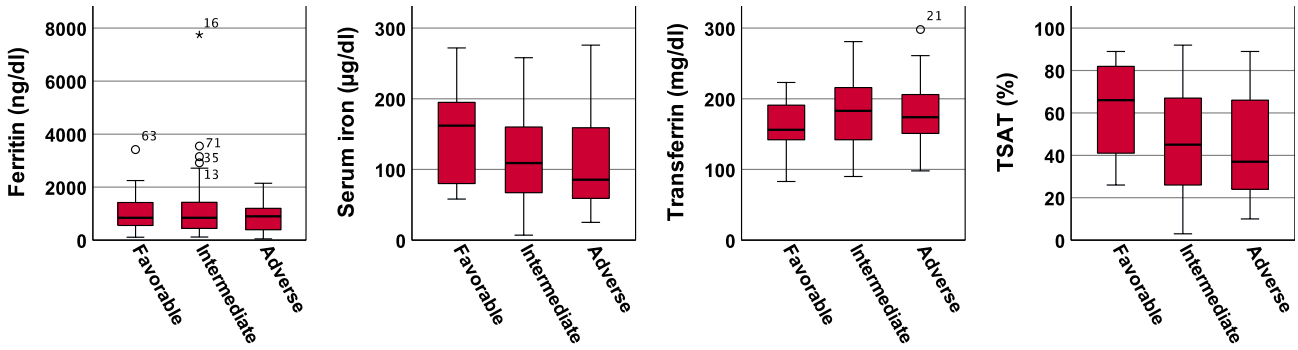

Supplemental Figure 1. Comparison of levels of ferritin, iron, transferrin and transferrin saturation (TSAT) in the sera of 84 AML patients (Supplemental Table 1), according to ELN risk subgroup (favorable, intermediate, adverse). No significance differences were detected.

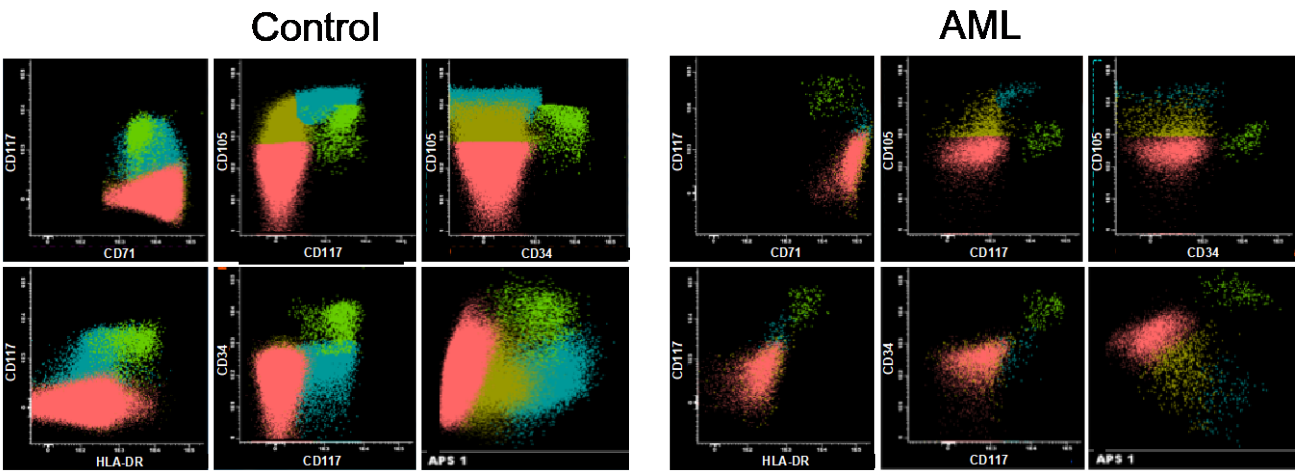

Supplemental Figure 2. Analysis of human bone marrow erythropoiesis in patients without (control) and with AML. Representative FACS plots showing different stages of human erythropoiesis. Ligh green dots: stage I nucleated red blood cells (NRBCs); blue dots: stage II NRBCs; dark green dots: stage III NRBCs; pink dots: stage IV NRBCs.

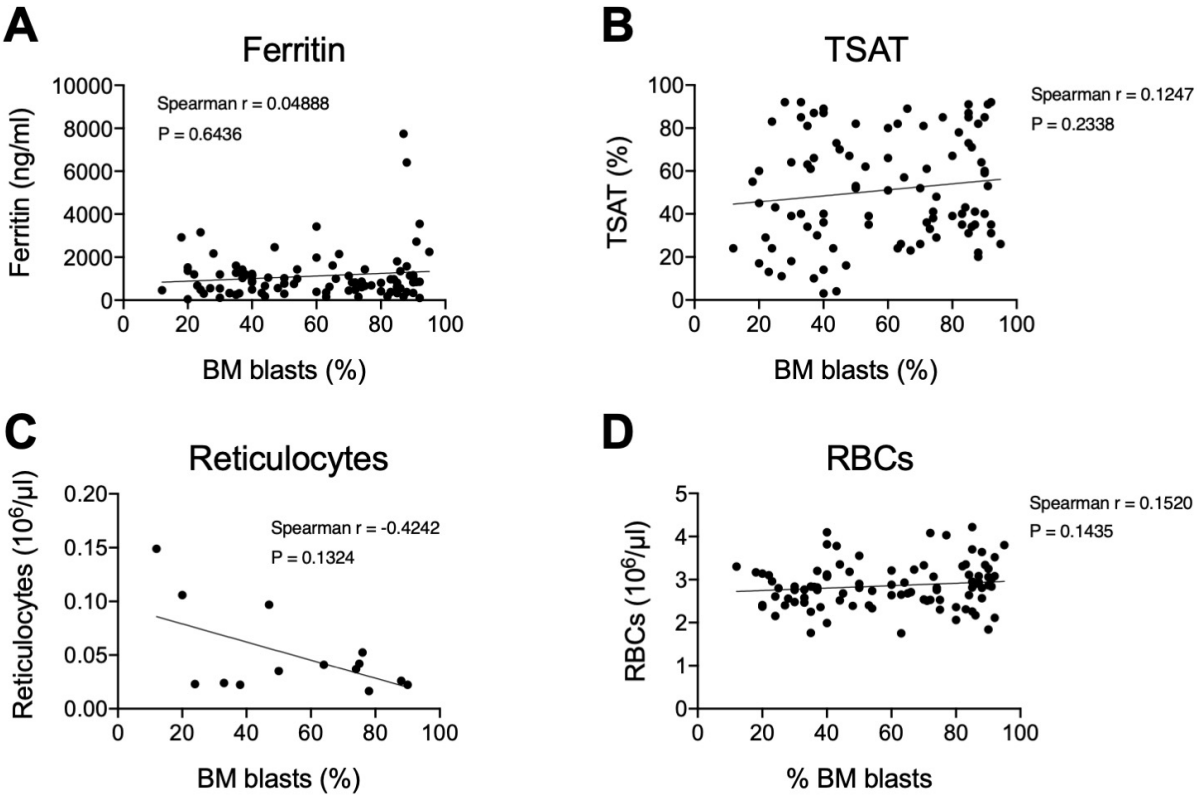

Supplemental Figure 3. Correlations between BM blast infiltration and iron or erythroid peripheral parameters. (A) Serum ferritin (n = 92), **(B)** serum transferrin saturation (TSAT) (n = 93), **(C)** peripheral blood reticulocyte counts (n = 14) and (D) peripheral red blood cell (RBC) counts (n = 94) as a function of bone marrow (BM) blast counts. Computed Spearman correlations and two-tailed P values are displayed.

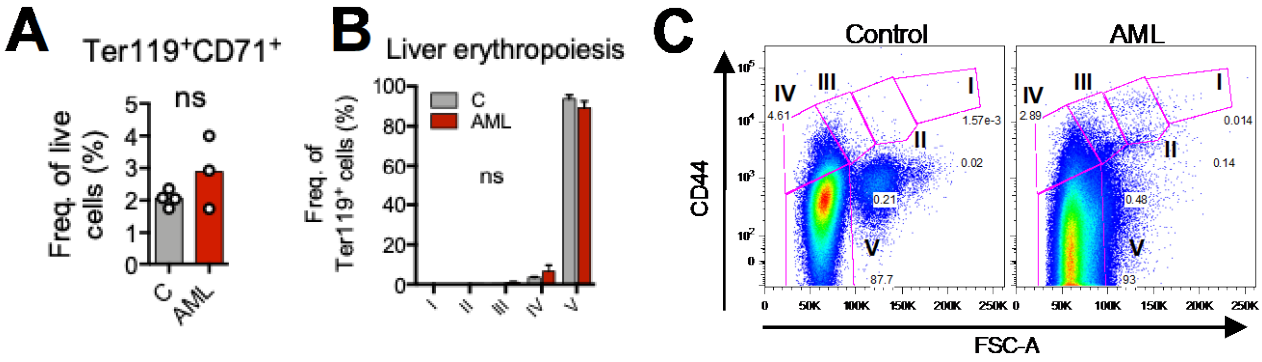

Supplemental Figure 4. Analysis of erythropoiesis in the liver. (A) Analysis of Ter119+CD71+ erythroid progenitors and **(B)** erythropoiesis stages revealed no significant differences between control and AML-burden mice. **(C)** Representative FACS plots of erythropoiesis stages in the liver. Data representative of 4 control and 3 leukemic mice.

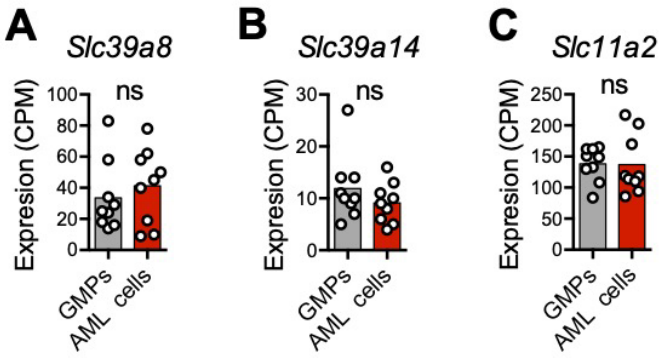

Supplemental Figure 5. Expression of NTBI transporters (ZIP8 and ZIP14) and DMT1 in AML cells. No significant differences were found in the expression of **(A)** *Slc39a8* (ZIP8 gene) **(B)** *Slc39a14* (ZIP14 gene) **(C)** *Slc11a2* (DMT1 gene) between non-malignant granulocyte-macrophage progenitors (GMPs) and AML cells (GSE105159). Each dot represents a mouse.

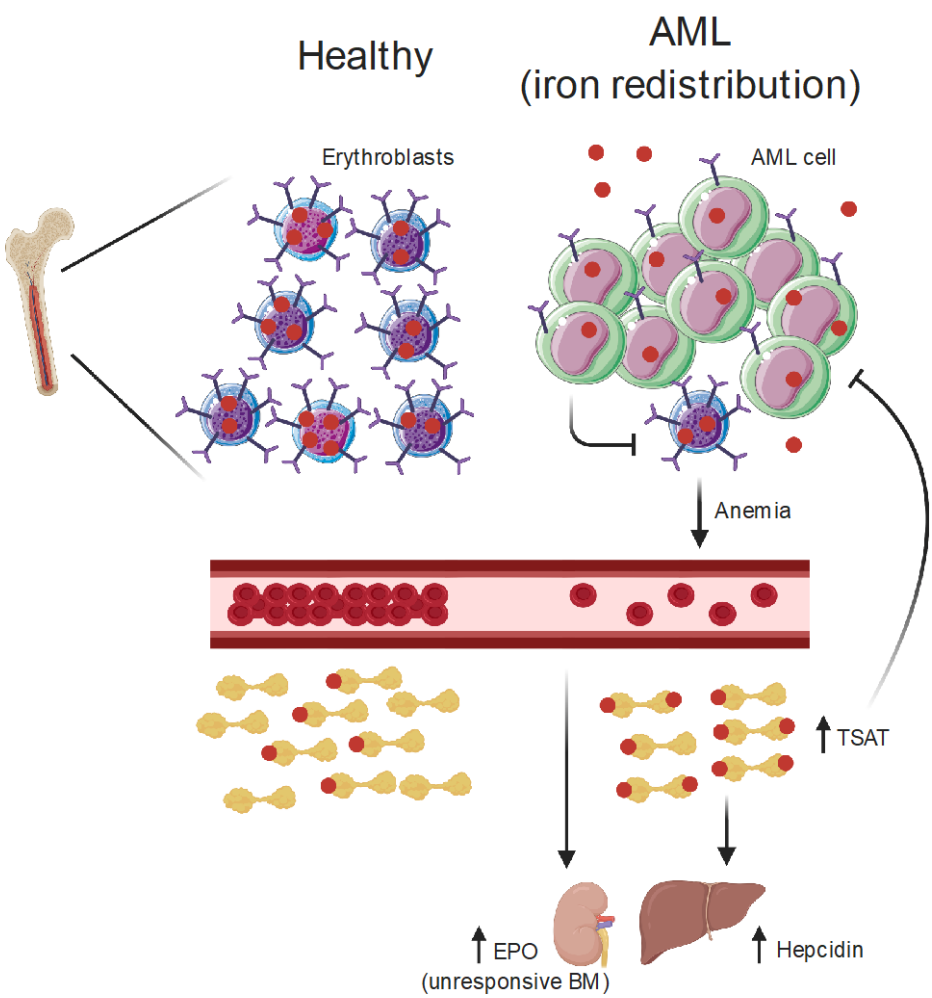

Visual Abstract. In contrast with healthy individuals, patients with AML have proliferation of leukemic cells in the bone marrow (BM) and consequently loss of $CD71^{hi}$ erythroblasts, which causes iron redistribution and increased transferrin saturation (TSAT). In parallel to increased hepcidin, there are increased levels of erythropoietin (EPO) due to anemia but the BM is unresponsive. Increased TSAT is also associated with better overall survival in AML. Created with BioRender.com

SUPPLEMENTAL TABLES

Supplemental Table 1. Baseline characteristics of 84 AML patients at diagnosis

Characteristics	
Gender, N (%)	
Male	48 (57,1)
Female	36 (42,9)
Median age, years (IQR)	62,5 (48,0-72,0)
Median Hb, g/dl (IQR)	8,7 (7,5-9,9)
Median WBC count, x10^9/l (IQR)	20,855 (7,260-45,558)
Median platelet count, x10^9/l (IQR)	42,00 (26,50-94,75)
Ferritin, ng/ml (IQR)	821,6 (445,1-1301,1)
Serum iron, µg/dl (IQR)	117 (70,0-175,8)
Transferrin, mg/dl (IQR)	173,0 (140,5-209,8)
TSAT, % (IQR)	51,5 (31,8-76,8)
Previous RBC transfusion, N (%)	23 (27,4)
Therapy, N (%)	
Intensive chemotherapy	54 (64,3)
Hypomethylating agent	6 (7,1)
Best supportive care	22 (26,2)
CR/CRi, N (%)	50 (59,4)
Cytogenetic Risk, N (%)	
Favorable	16 (19,0)
Intermediate	56 (66,7)
Adverse	10 (11,9)
AML subtype, N (%)	
de novo AML	70 (83,3)
Secondary AML	14 (16,7)
WHO classification 2016, N (%)	
AML with recurrent genetic abnormalities	
AML with t(8;21)(q22;q22.1); RUNX1-RUNX1T1	3 (3,6)
AML with inv(16)(p13.1q22) or t(16;16)(p13.1;q22); CBFB-MYH11	7 (8,3)
AML with t(9;11)(p21.3;q23.3);MLLT3-KMT2A	1 (1,2)
AML with inv(3)(q21.3q26.2) or t(3;3)(q21.3;q26.2); GATA2, MECOM	2 (2,4)
Provisional entity: AML with BCR-ABL1	1 (1,2)
AML with mutated NPM1	22 (26,2)
AML with myelodysplasia-related changes	21 (25,0)
Therapy-related myeloid neoplasms	2 (2,4)
AML, NOS	
AML without maturation	3 (3,6)
AML with maturation	6 (7,1)
Acute myelomonocytic leukemia	4 (4,8)
Acute monoblastic/monocytic leukemia	6 (7,1)
Pure erythroid leukemia	1 (1,2)
Not classified	5 (6,0)

N - number of observations; IQR - interquartile range; Hb - hemoglobin; WBC - peripheral white blood cell count; CR - complete response; CRi - complete response with incomplete blood count recovery.

Supplemental Table 2. Baseline characteristics of 29 rheumatological patients with anemia of inflammation

Characteristics	
Gender, N (%)	
Male	9 (31)
Female	20 (69)
Median age, years (IQR)	57,0 (48,5-72,0)
Median Hb, g/dl (IQR)	11,4 (10,9-11,9)
Median WBC count, x10^9/l (IQR)	7,240 (5,260-9,650)
Median platelet count, x10^9/l (IQR)	258,00 (210,50-318,25)
Ferritin, ng/ml (IQR)	38,7 (17,8-119,9)
Serum iron, µg/dl (IQR)	37,0 (28,0-49,0)
Transferrin, mg/dl (IQR)	294,0 (244,0-355,5)
TSAT, % (IQR)	9,0 (6,0-13,0)
Oral iron treatment, N (%)	9 (31,0)
Diagnosis, N (%)	
Juvenile idiopathic arthritis	1 (3,4)
Rheumatoid arthritis	15 (51,7)
Psoriatic arthritis	5 (17,2)
Systemic lupus erythematosus	4 (13,8)
Behçet's disease	1 (3,4)
Ankylosing spondylitis	2 (6,9)
Sjögren syndrome	1 (3,4)

N - number of observations; IQR - interquartile range; Hb - hemoglobin; WBC - peripheral white blood cell count.

Supplemental Table 3. Characteristics of hematological patients at diagnosis

Group	ID	Diagnosis	Age	Sex	Cytogenetics	Molecular Genetics
Control	DC07	Folicular Lymphoma	44	F		
	DC10	B ALL in remission	63	F		
	DC14	NHL MALT	50	M		
	DC16	Folicular Lymphoma	51	M		
	DC22	NHL MALT	78	F		
	DC23	NHL DLBCL	45	M		
	DC24	MCL	83	M		
	DC25	NHL MALT	45	F		
	DC28	Sarcoidosis	59	F		
	DC29	NHL MALT	51	F		
	DC30	Folicular Lymphoma	70	F		
	DC31	NHL MALT	54	M		
AML	DC01	De novo AML	69	F	46,XY	IDH1/2-
	DC02	De novo AML	65	F	47,XX,+8[2]/47,idem,t(3;21)(p25;q22)[18]	FLT3-ITD+
	DC03	De novo AML	22	M	46,XY,inv(16)(p13q22)[20]	CBFB-MYH11+/ FLT3-ITD+
	DC04	De novo AML	64	F	No metaphases	
	DC06	De novo AML	57	F	46,XX[20]	FLT3-ITD-
	DC08	De novo AML	69	F	46,XX[8]	FLT3-ITD-
	DC17	AML secundary to MDS/MPN	62	F	46,XX,add(3)(q12),add(18)(q23)x2[6]	FLT3-ITD-
	DC18	De novo AML	53	M	44~46,XY,add(11)(q23),inc[4]	
	DC20	De novo AML	48	M	45,X,-Y,t(8;21)(q22;q22),del(9)(q21q34)[20]	RUNX1-RUNX1T1+
	DC26	De novo AML	57	M	46,XY[20]	
	DC32	De novo AML	60	M	45~46,XY,i(1)(p10),-4,add(4)(p12),-5,add(7)(q32),+8,add(14)(p11.2),-15,-16,-17,i(21)(q10),+4mar[cp18]/46,XY[2]	

ALL – acute lymphoblastic leukemia; NHL – non-Hodgkin lymphoma; MALT – mucosa-associated lymphoid tissue; MCL – mantle cell lymphoma; MDS – myelodysplastic syndrome; MPN – myeloproliferative neoplasm.

Supplemental Table 4. Characteristics of patients who underwent analysis of bone marrow nucleated red blood cells

Group	Diagnosis	Age	Sex
Control	Multiple myeloma - 2 months after autologous HSC transplantation	61	M
	Anemia in characterization	76	F
	Allogeneic HSC transplantation post AML	58	M
	Relapse of Diffuse Large B-Cell Lymphoma	81	M
AML	De novo AML with 5q-	48	M
	De novo AML with normal karyotype	84	M
	De novo AML with trisomy 8	54	F
	De novo AML with t(15;17)	72	M
	De novo AMKL with der(9)t(1;9)	49	F
	De novo AML with normal karyotype	58	F

HSC – hematopoietic stem cell; AMKL – acute megakaryoblastic leukemia.

Supplemental Table 5. Multivariate Cox regression on overall survival of all 84 AML patients (Supplemental Table 1)

	Overall Survival		
Variable	HR	95% CI	P
Age (>60 vs. ≤60 years)	4,729	2,044-10,941	**<0,001**
ELN 2017 (intermediate vs. favorable risk)	0,950	0,347-2,602	0,921
ELN 2017 (favorable vs. adverse risk)	2,198	0,636-7,605	0,213
AML subtype (de novo vs. secondary)	0,663	0,212-2,071	0,479
TSAT (≤51,5 vs. >51,5%)	2,779	1,223-6,312	**0,015**
Response to induction (CR vs. no CR)	1,992	0,742-5,344	0,171

ELN – European Leukemia Net; TSAT – transferrin saturation; CR – complete response; HR – hazard ratio; CI – confidence interval; Bold: significant P values ($p<0.05$)

Supplemental Table 6. Multivariate Cox regression on overall survival of the AML patients who underwent intensive chemotherapy (Supplemental Table 1)

	Overall Survival		
Variable	HR	95% CI	P
Age (>60 vs. ≤60 years)	4,699	2,030-10,877	**<0,001**
ELN 2017 (intermediate vs. favorable risk)	0,955	0,348-2,621	0,928
ELN 2017 (favorable vs. adverse risk)	2,082	0,589-7,363	0,255
AML subtype (de novo vs. secondary)	0,683	0,216-2,157	0,516
TSAT (≤51,5 vs. >51,5%)	2,703	1,172-6,234	**0,020**
Response to induction (CR vs. no CR)	1,946	0,712-5,319	0,194

ELN – European Leukemia Net; TSAT – transferrin saturation; CR – complete response; HR – hazard ratio; CI – confidence interval; Bold: significant P values ($p<0.05$)